



New quantitative indices of cardiac amyloidosis with ^{99m}Tc -pyrophosphate scintigraphy

Noritake Matsuda¹ · Hideki Otsuka² · Tamaki Otani³ · Shota Azane¹ · Yamato Kunikane¹ · Yoichi Otomi⁴ · Yuya Ueki⁵ · Masahiro Kubota⁶ · Masafumi Amano¹ · Shusuke Yagi⁷ · Masataka Sata⁷ · Masafumi Harada⁴

Received: 6 September 2022 / Accepted: 15 November 2022 / Published online: 30 November 2022
© The Author(s) under exclusive licence to Japan Radiological Society 2022

Abstract

Purpose Amyloid light chain (AL) and transthyretin (ATTR) are the major subtypes of cardiac amyloidosis (CA). ^{99m}Tc -pyrophosphate (PYP) scintigraphy is used to differentiate ATTR from other CA subtypes. We adapted the standardized uptake value (SUV) for ^{99m}Tc -PYP and proposed two quantitative indices, amyloid deposition volume (AmyDV) and total amyloid uptake (TAU). This study aimed to evaluate the utility of these quantitative indices in differentiating ATTR from non-ATTRs.

Materials and methods Before the SUV measurement, the Becquerel calibration factor (BCF) of ^{99m}Tc was obtained by a phantom experiment. Thirty-two patients who had undergone hybrid SPECT/CT imaging 3 h after injection of ^{99m}Tc -PYP (370 MBq) were studied. CT attenuation correction for image reconstruction was applied in all. We calculated SUV, AmyDV, and TAU using a quantitative analysis software program for bone SPECT (GI-BONE) and analyzed AmyDV using two methods: threshold method (set 40%); and constant value method (average SUV_{max} of ribs). We assessed the diagnostic ability of heart-to-contralateral lung (H/CL) ratio, SUV, AmyDV, and TAU to differentiate ATTR from non-ATTR using receiver operating characteristic (ROC) analysis.

Results Statistically significant differences in all quantitative indices were observed between ATTR and non-ATTR. The area under the curve of each quantitative index for discriminating between ATTR and non-ATTR were as follows: H/CL, 0.997; SUV_{max} , 0.953; SUV_{mean} (M1), 0.964; SUV_{mean} (M2), 0.969; AmyDV (M1), 0.875; AmyDV (M2), 0.974; and TAU, 0.974. The AmyDV (M2) had higher diagnostic ability than AmyDV (M1). Thus, TAU was calculated as $\text{AmyDV (M2)} \times \text{SUV}_{\text{mean}}$ (M2). In the ROC curve, SUV, AmyDV, and TAU had almost the same diagnostic ability as H/CL in distinguishing ATTR from non-ATTRs.

Conclusions We propose two novel 3D-based quantitative parameters (AmyDV and TAU) that have almost equal ability to discriminate ATTR from non-ATTR.

Keywords Cardiac amyloidosis (CA) · Standardized uptake value (SUV) · Amyloid deposition volume (AmyDV) · Total amyloid uptake (TAU) · Becquerel calibration factor (BCF)

✉ Hideki Otsuka
hideki.otsuka@tokushima-u.ac.jp

¹ Department of Radiology, Tokushima University Hospital, Kuramoto-Cho 2-50-1, Tokushima 770-8503, Japan

² Department of Medical Imaging/Nuclear Medicine, Tokushima University Graduate School of Biomedical Sciences, Tokushima, Japan

³ Advance Radiation Research, Education and Management Center, Tokushima University, Tokushima, Japan

⁴ Department of Radiology and Radiation Oncology, Tokushima University Graduate School of Biomedical Sciences, Tokushima, Japan

⁵ Tokushima University Graduate School of Biomedical Sciences, Tokushima, Japan

⁶ Department of Radiology, Tokushima Red Cross Hospital, Tokushima, Japan

⁷ Department of Cardiovascular Medicine, Tokushima University Graduate School of Biomedical Sciences, Tokushima, Japan

Introduction

Amyloid light chain (AL) and transthyretin (ATTR) are major subtypes of cardiac amyloidosis (CA) [1]. ^{99m}Tc -pyrophosphate (PYP) scintigraphy demonstrates selective positive uptake in ATTR CA and has been used to differentiate ATTR from other CA subtypes. Myocardial uptake of ^{99m}Tc -PYP is analyzed visually and quantitatively. In a visual evaluation, uptake by heart is compared with that by ribs and graded: grade 0, none by heart but normal in ribs; grade 1, less than rib uptake; grade 2, equal to rib uptake; grade 3, more than rib uptake. Grade 2 and 3 are judged as positive for ATTR.

In the quantitative analysis, the uptake ratio of the heart to the contralateral lung (H/CL), was calculated on the planar images. $\text{H/CL} > 1.5$ was judged as positive [2–5].

The standardized uptake value (SUV) was first introduced for positron emission tomography (PET) and is the most commonly used quantitative index for PET, but rarely used for SPECT. Quantitative evaluation using the SUV is thus an advantage of PET over SPECT. Software program which can calculate the SUV, perform quantitative analysis of bone SPECT/CT and evaluation of the uptake has been developed and implemented. We adapted the SUV for ^{99m}Tc -PYP and proposed two quantitative indices, amyloid deposition volume (AmyDV) and total amyloid uptake (TAU), corresponding to the volume of abnormal myocardial amyloid deposition. This study aimed to evaluate the utility of these quantitative indices in differentiating ATTR from non-ATTRs.

Materials and methods

This single center, retrospective study was performed at our institution, after approval by the ethics committee. Requirement of written informed consent was waived. The information disclosure document for this study is available to the public on our institution website. We performed phantom and clinical studies using a hybrid SPECT/CT system (Symbia T16; Siemens, Germany).

Phantom study

Before the SUV measurement, we performed a phantom experiment to calculate the Becquerel calibration factor (BCF) for converting counts of reformatted SPECT images to the radioactivity concentration. A cylindrical phantom (inner diameter, 16 cm; length, 15 cm; volume, 3016 mL; Sangyo Kagaku, Tokyo, Japan) was prepared with water

and 21.4 MBq of ^{99m}Tc -PYP. We scanned the phantom for 15 min and reconstructed the data according to the clinical ^{99m}Tc -PYP SPECT/CT protocol (Table 1). The BCF acquired using bone SPECT analysis software, GI-BONE (AZE Corp., Tokyo, Japan), was used to calculate the SUV in this study.

Patient study

We studied 32 patients who underwent ^{99m}Tc -PYP scintigraphy at our hospital between April 2018 and June 2022 in this retrospective study (ATTR, $n = 8$; non-ATTR, $n = 24$; men, $n = 23$; women, $n = 9$; age, 16–83 years; Table 2). Clinical diagnosis was confirmed by board-certified cardiologists. Cardiac biopsy was performed in 12 amyloidosis patients, of whom 5 were pathologically proven to be ATTR type, and 7 to be AL type. In every patient, approximately 370 MBq of ^{99m}Tc -PYP was injected intravenously, a whole-body planar image was obtained, and the SPECT/CT scan was performed 3 h after injection. We used CT data for attenuation correction and anatomical information. Imaging after 1 h improves sensitivity, and imaging after 3 h improves specificity [6]. The visual assessment method is a validated technique for images obtained after 3 h, but the same criteria should not be applied to images obtained after 1 h because it is sometimes difficult to distinguish between a blood radioisotope pool and myocardial uptake. At our hospital, both visual and quantitative evaluation have been performed, and only planar imaging after 3 h, which has high specificity, and SPECT/CT examinations are performed.

Visual evaluation

The 4-score grading of cardiac uptake was performed by two board-certified nuclear medicine specialists.

- 0: No myocardial uptake. Normal ribs uptake.
- 1: Lower myocardial uptake than ribs uptake.

Table 1 Image processing

SPECT/CT scanner	Symbia T16 (Siemens)
RI	^{99m}Tc -PYP
Collimator	LEHR
keV	140 keV \pm 15%
Matrix	128 \times 128
Pixel size	3.3 mm
Image processing	Continuous mode
Rotation	180°
Collection time	30 s \times 30
Attenuation correction	CTAC

Table 2 Patient characteristics

	ATTR	Non-ATTR	<i>p</i> value
Number of patients	8	24	–
Men/women	8/0	15/9	< 0.05
Age: mean (range)	76.1 (69–83)	63.6 (16–83)	< 0.05
Body weight: mean (SD)	57.4 (3.48)	60.9 (17.1)	0.363
	AL		12
	Heart failure with preserved ejection function: HFpEF		3
	Hypertensive heart disease		2
	Dilated cardiomyopathy: DCM		1
	Hypertrophic cardiomyopathy: HCM		1
	Mitochondrial cardiomyopathy		1
	Duchenne muscular dystrophy		1
	Chronic heart failure		1
	Congestive heart failure: CHF		1
	No heart disease		1

2: Myocardial uptake equivalent to ribs uptake.

3: Higher myocardial uptake than ribs uptake with mild/absent rib uptake.

Quantitative indices

Heart to contralateral lung (H/CL) ratio

The H/CL ratio was calculated using Syngo MI (SIEMENS Healthineers, Germany). On the planar images, identical regions of interest (ROI) were marked on the heart and contralateral chest, and the heart/contralateral (H/CL) ratio calculated as a ratio of the heart ROI counts to the contralateral chest ROI counts (Fig. 1).

SUV

The radiation count was converted to radioactivity using the BCF calculated with the quantification software program for bone SPECT (GI-BONE; AZE Corp., Tokyo, Japan). Its formula is: Radioactivity of the region (Bq) = (radiation count of the region) × BCF.

The SUV was calculated using the formula: $SUV = \text{mean volume of interest (VOI) activity (MBq/g)} / [\text{injected dose (MBq)} / \text{body weight (g)}] = [(\text{total count of VOI}) \times \text{BCF} / \text{the volume of VOI}] / [\text{injected dose} / \text{body weight}]$.

The SUV of the heart and ribs were measured separately using the previous BCF. To set the VOI, 40% of the SUV_{max} of the VOI, which is the default value of GI-BONE, was used as the threshold. The SUV_{max} , SUV_{peak} , and SUV_{mean} of the heart and SUV_{max} of the ribs were calculated. The entire heart was set as its VOI, avoiding the ribs and spine. The VOIs of the ribs were set on the right-side ribs, and the

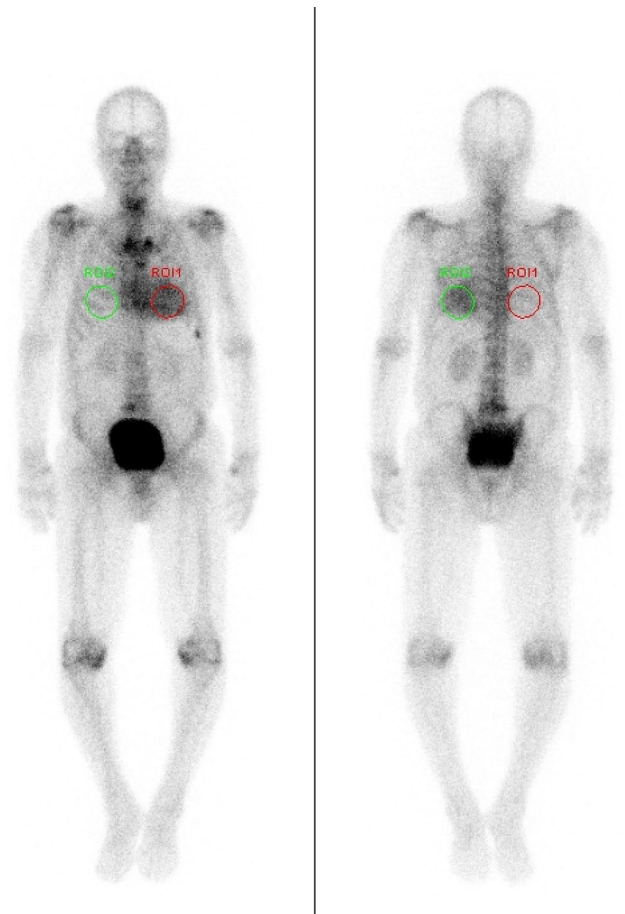


Fig. 1 H/CL ratio – ATTR patient: ROI 1; The average count is 52.39. ROI 2; The average count is 26.56. H/CL=1.97. Intense uptake in myocardium is observed compared to ribs (grade 3)

highest SUV was considered the SUV_{max} of the ribs of each patient. Focal intense uptake suggestive of a rib fracture was excluded (Fig. 2).

We proposed two quantitative indices for ^{99m}Tc -PYP: AmyDV and TAU.

Amyloid deposition volume (AmyDV)

Amyloid deposition volume corresponds to the metabolic tumor volume (MTV) on FDG-PET. It represents the volume of voxels with an SUV exceeding the cut-off value. The region exceeding the cut-off value was considered amyloid deposition. We analyzed AmyDV by two methods:

threshold method, M1 (set 40%); and constant value method, M2 (average of ribs SUV_{max} from all the patients) (Fig. 3).

The diagnostic abilities of each method in differentiating ATTR from non-ATTRs were assessed using receiver operating characteristic (ROC) analysis and the area under the curve (AUC).

Total amyloid uptake (TAU)

The cut-off value that had the highest AUC for AmyDV was adapted to calculate TAU.

Total amyloid uptake corresponds to total lesion glycolysis (TLG) on FDG-PET. The TAU was calculated using the following formula:

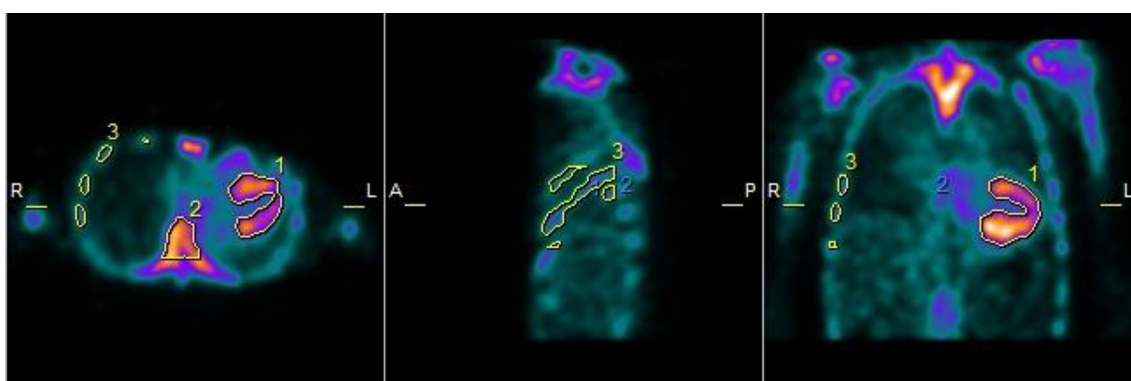


Fig. 2 Setting VOI for myocardium and ribs

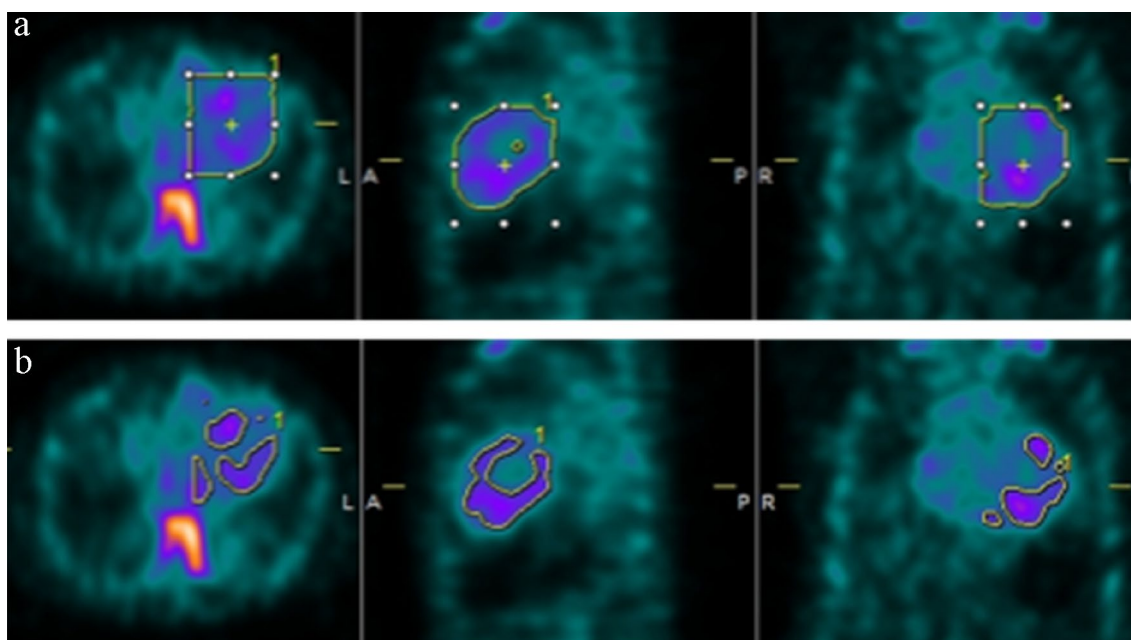


Fig. 3 Two analysis methods for AmyDV. **a** M1, threshold method (set 40%). **b** M2, constant value method (average of ribs SUV_{max} from all patients)

$$\text{TAU} = \text{AmyDV} \times \text{SUV}_{\text{mean}}$$

The diagnostic abilities of the H/CL ratio, SUV_{max} , SUV_{peak} , SUV_{mean} , AmyDV, and TAU in differentiating ATTR from non-ATTRs were also assessed using ROC analysis and the AUC.

Statistical analysis

We used the chi-squared test and Student's *t*-test to compare patient characteristics such as sex, age, and body weight. The Student's *t*-test was used to compare each index (H/CL ratio, SUV_{max} , SUV_{peak} , SUV_{mean} , AmyDV, and TAU) between the ATTR and non-ATTR groups. Statistical significance was set at $p < 0.05$.

We used the ROC curve analysis to set the cut-off value and evaluate the sensitivity, specificity, test accuracy, and AUC of each quantitative index. The difference in the AUC was examined using the chi-squared test.

Results

Phantom study

The BCF was obtained as 4858.926 [Bq/cps].

Visual evaluation

Two nuclear medicine specialists interpreted the planar and SPECT images independently. The issue of same images graded differently by the specialists were resolved through consensus to provide a final grade. The results are presented in Table 3. Grade 2 or 3 were considered ATTR positive. None of the non-ATTR cases was classified as grade 3.

Quantitative indices

The average of the ribs SUV_{max} from all 32 patients was 2.1 ± 1.0 .

The statistical results of the ROC analysis for cardiac SUV_{mean} and AmyDV are shown in Fig. 4 and Table 4, respectively, for comparison between M1 and M2 when TAU was calculated. For cardiac SUV_{mean} , there was no statistically significant difference depending on the threshold-setting method. For AmyDV, M2 (constant value method) was statistically superior to M1 (threshold method) and had a higher AUC (0.974). TAU was calculated using the following formula:

$$\text{TAU} = \text{AmyDV (M2)} \times \text{SUV}_{\text{mean (M2)}}$$

Table 3 Grade classification

	ATTR (<i>n</i> =8)	non-ATTR (<i>n</i> =24)	Total (<i>n</i> =32)
Planar			
Grade classification			
0	0	11	11
1	0	12	12
2	0	1	1
3	8	0	8
Quantitative SPECT			
Grade classification			
0	0	19	19
1	0	4	4
2	1	1	2
3	7	0	7

The six quantitative indices are listed in Table 5. All index values were significantly higher in the ATTR group ($P < 0.05$), than those in the non-ATTR group.

Figure 5 and Table 6 show the ROC results of the diagnostic ability of differentiating ATTR from non-ATTR. The SUV_{mean} and AmyDV were calculated using M2. The sensitivity, specificity, and accuracy of SUV_{max} , SUV_{peak} , SUV_{mean} , AmyDV, and TAU were slightly inferior to those of H/CL. The AUC showed almost the same values for SUV_{max} (0.953), SUV_{peak} (0.943), SUV_{mean} (0.969), AmyDV (0.974), TAU (0.974), and H/CL (0.997).

Discussion

Amyloidosis is the deposition of abnormal proteins in various tissues and organs causing their dysfunction and even failure. The reported frequency of AL amyloidosis in the United States was 40.5 per million in 2015 [7]. The deposition of senile systemic ATTR-derived amyloid fibers in tissues progresses with age and a clinicopathological autopsy study reported that approximately 25% of people over 80 years old had amyloid deposits in the heart [8, 9].

Magnetic resonance imaging (MRI), CT, and nuclear medicine imaging have been used to diagnose CA. Diagnostic uses of Cine MRI and delayed-enhanced MRI are common, but lately, the usefulness of myocardial T1 mapping for quantitative evaluation of myocardial tissue has been shown and recommended for the diagnosis of CA [10, 11]. T2 mapping and myocardial strain MRI have also been found useful [12, 13].

In nuclear medicine examinations, $^{99\text{m}}\text{Tc}$ -PYP bone scintigraphy, also has high sensitivity and specificity for ATTR CA and is used for noninvasive pathological diagnosis [6, 14, 15]. The mechanism of accumulation of bone tracers,

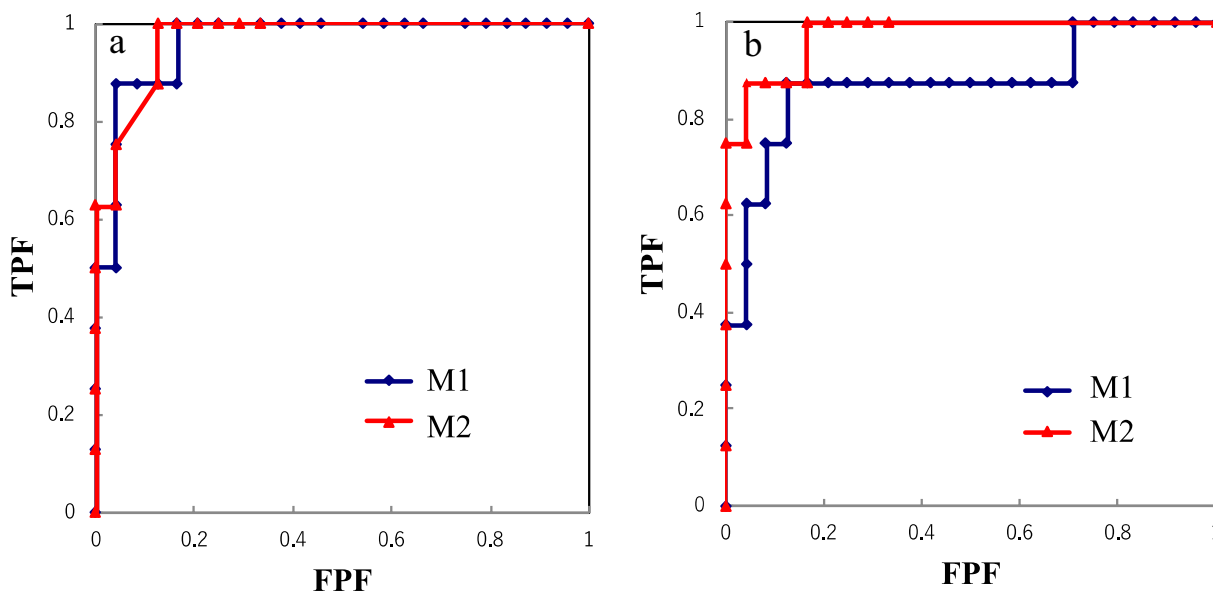


Fig. 4 ROC analysis for cardiac SUVmean and AmyDV. **a** ROC curve of cardiac SUVmean (blue line: M1, red line: M2). **b** ROC curve of AmyDV (blue line: M1, red line: M2)

Table 4 ROC analysis (value)

	Sensitivity [%]	Specificity [%]	Cut-off value	AUC	Accuracy [%]
Cardiac SUVmean					
M1	100	99.8	1.3	0.964	81.3
M2	100	100	2.2	0.969	84.4
AmyDV					
M1	87.5	99.9	425	0.875	87.5
M2	100	99.8	1	0.974	87.5

**p* < 0.05 in comparison to non-ATTR

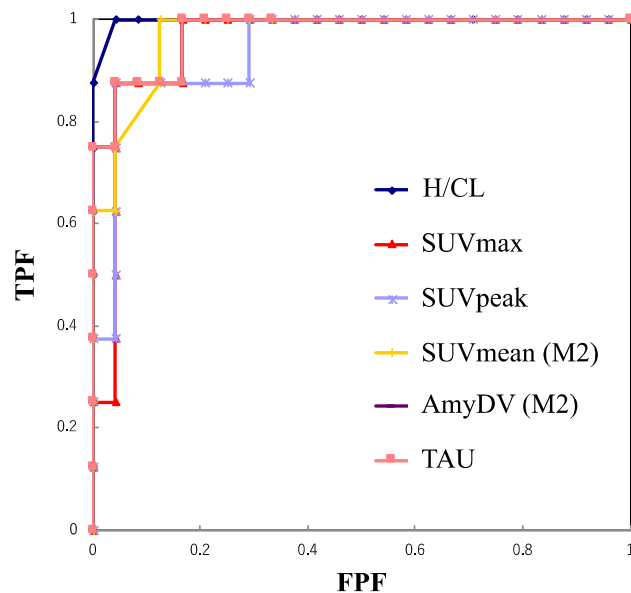
including ^{99m}Tc-PYP, in ATTR CA is currently unknown; however, a calcium-mediated mechanism has been speculated. ¹²³I-meta-iodobenzylguanidine (¹²³I-MIBG) is useful for detecting denervation in CA and assessing the pathophysiology of heart failure [16]. In recent years, amyloid PET using an amyloid-specific tracer has also been studied at the preclinical stage [17–19]. Identification of CA non-invasively, as either AL or ATTR, is important as their treatment protocols are different. It is difficult to distinguish AL from ATTR using cardiovascular MRI (CMR) and CT. The sensitivity of endomyocardial biopsy for ATTR CA was reported to be 100%, and the frequency of sampling errors was extremely low [20]. However, endomyocardial biopsy is highly invasive, and the detection rate of amyloid protein is not high in abdominal fat aspiration of wild-type ATTR amyloidosis [21]. ^{99m}Tc-PYP scintigraphy is a highly useful and less invasive method of detecting ATTR CA. We used visual grading and H/CL ratio to evaluate cardiac uptake in ^{99m}Tc-PYP scintigraphy and proposed two new quantitative indices in this study.

The results in Fig. 5 and Table 6 show that, SUV_{max}, SUV_{peak}, SUV_{mean}, AmyDV, and TAU were as useful as the H/CL ratio. The most widely used method for distinguishing ATTR CA and AL CA by visual comparison of the ribs and myocardium in ^{99m}Tc-PYP scintigraphy was developed by Perugini et al. [3]. The H/CL method of semi-quantitative evaluation of the ^{99m}Tc-PYP uptake by heart uses the count ratio. Chao et al. found that with ^{99m}Tc-PYP quantitative SPECT integrated with adjustable partial volume correction (PVC) factors, it is feasible to quantitatively and objectively assess the burden of cardiac amyloidosis for the diagnosis of ATTR CA. For quantitative SPECT, phantom studies were initially performed to determine the image conversion factor (ICF) and PVC factor to recover ^{99m}Tc-PYP activity concentration in the myocardium and calculate the standardized uptake value (SUV). The SUV_{max} was compared among groups of ATTR CA, AL CA, and so on and among categories of Perugini visual scores (grades 0–3) [22]. The GI-BONE was developed for bone SPECT and calculates SUV and

Table 5 Range and mean \pm standard deviation of each quantitative index

Quantitative index		ATTR ($n=8$)	non-ATTR ($n=24$)
H/CL ratio	Range	1.64–1.98	0.82–1.64
	Mean \pm SD	1.82 \pm 0.11*	1.17 \pm 0.15
SUV _{max}	Range	2.3–4.5	1.3–4.0
	Mean \pm SD	3.4 \pm 0.8*	2.0 \pm 0.5
SUV _{peak}	Range	2.1–4.2	1.3–3.5
	Mean \pm SD	3.1 \pm 0.7*	1.9 \pm 0.5
SUV _{mean}	Range	1.3–2.5	0.8–1.9
	Mean \pm SD	1.9 \pm 0.5*	1.1 \pm 0.2
M2	Range	2.2–2.8	0.0–2.3
	Mean \pm SD	2.4 \pm 0.2*	0.7 \pm 1.0
AmyDV	Range	185–976	35–556
	Mean \pm SD	543 \pm 214*	271 \pm 123
M2	Range	1–477	0–40
	Mean \pm SD	185 \pm 169*	2 \pm 8
TAU	Range	1–1323	0–94
	Mean \pm SD	488 \pm 468*	5 \pm 19

* $p < 0.05$ in comparison to non-ATTR

**Fig. 5** ROC curve analysis for quantitative index

uptake volume. In calculating SUV_{mean} and AmyDV, two

methods were examined to evaluate significant uptake. In M1, when the maximum value is 100%, 40% or more is VOI; therefore, it is possible that the VOI contains the accumulation of the cardiac pool and the low uptake part. M1 was considered inappropriate because there was a significant difference in the evaluation of uptake among individuals. In M2, the average SUV_{max} of the ribs was used as the threshold value because the case of higher myocardial uptake than rib uptake in the visual evaluation was positive. Therefore, M2 was considered suitable for calculating SUV_{mean}, AmyDV, and TAU. The SUVs quantitatively evaluated the degree of ^{99m}Tc-PYP uptake, and AmyDV quantitatively evaluated the volume of amyloid deposition. Total amyloid uptake is a quantitative index with characteristics of both SUV and AmyDV. H/CL is a simple and well-established parameter which uses planar images. AmyDV and TAU have the same ability as H/CL to distinguish between ATTR and non-ATTRs. However, they have an advantage over H/CL in that they can be evaluated as a 3D-based parameter. H/CL is the relative ratio of the heart-to-contralateral chest, whilst AmyDV and TAU are more quantitative and may be useful to monitor changes in amyloid deposition volume during disease progression or follow-up. Another advantage is that the ROI setting of H/CL is affected by the degree of rib inclusion, whereas the new indices we propose are not affected by this factor.

Every institution can assess this method with reference to the original BCF of the gamma camera and with the introduction of analytical software. This study had some limitations. Being a single center study, the patient population was limited. A multicenter study with a larger population is necessary to confirm the utility of the new TAU index with GI-BONE in reference to the original BCF of each institution. The calibration of gamma camera systems is also necessary to normalize and standardize the method.

Conclusion

AmyDV and TAU showed diagnostic abilities to distinguish ATTR from non-ATTRs that were nearly identical to that of H/CL. Therefore, AmyDV and TAU are novel 3D-based parameters of ATTR deposition that can be used to assess the severity of the disease and monitor its progression.

Table 6 ROC analysis

Quantitative index	Sensitivity [%]	Specificity [%]	Cut-off value	AUC	Accuracy [%]
H/CL	100	99.9	1.64	0.997	96.9
SUVmax	100	99.8	2.3	0.953	81.3
SUVpeak	87.5	99.9	2.5	0.943	93.8
SUVmean	100	99.9	2.2	0.969	84.4
AmyDV	100	99.8	1	0.974	87.5
TAU	100	99.8	1	0.974	84.4

Author contributions HO conceived the idea of the study. NM performed all phantom experiments, clinical data analysis, and described this article. HO and YO interpreted the planar and SPECT images individually. TO, SA, YK, and MA performed the phantom experiment and clinical nuclear medicine examination with technical advice. YU and KM performed the phantom experiment. MS and SY performed clinical diagnosis and suggestion of cardiac disease pathologies. MH performed clinical suggestion. All authors read and approved the final manuscript.

Data availability The data that support the findings of this study are available on request from the corresponding author, [HO]. The data are not publicly available due to their containing information that could compromise the privacy of research participants.

Declarations

Conflict of interest The authors declare that they have no competing interests.

Ethical approval This retrospective study was performed at a single university hospital and received approval from the Tokushima University Hospital ethics committee (approval number: 3947).

Informed consent The requirement of written informed consent was waived.

Consent for publication The information disclosure document of this study is available to the public on Tokushima University Hospital website.

References

- Tuzovic M, Yang EH, Baas AS, Depasquale EC, Deng MC, Cruz D, et al. Cardiac amyloidosis: diagnosis and treatment strategies. *Curr Oncol Rep*. 2017;19:46. <https://doi.org/10.1007/s11912-017-0607-4>.
- Hutt DF, Quigley AM, Page J, Hall ML, Burniston M, Gopaul D, et al. Utility and limitations of 3,3-diphosphono-1,2-propanodicarboxylic acid scintigraphy in systemic amyloidosis. *Eur Heart J Cardiovasc Imaging*. 2014;15:1289–98. <https://doi.org/10.1093/ehjci/jeu107>.
- Perugini E, Guidalotti PL, Salvi F, Cooke RM, Pettinato C, Riva L, et al. Noninvasive etiologic diagnosis of cardiac amyloidosis using ^{99m}Tc-3, 3-diphosphono-1, 2-propanodicarboxylic acid scintigraphy. *J Am Coll Cardiol*. 2005;46:1076–84. <https://doi.org/10.1016/j.jacc.2005.05.073>.
- Bokhari S, Castaño A, Pozniakoff T, Deslisle S, Latif F, Maurer MS. (99m)Tc-pyrophosphate scintigraphy for differentiating light-chain cardiac amyloidosis from the transthyretin-related familial and senile cardiac amyloidoses. *Circ Cardiovasc Imaging*. 2013;6:195–201. <https://doi.org/10.1161/CIRCIMAGING.112.000132>.
- Gertz MA, Brown ML, Hauser MF, Kyle RA. Utility of technetium Tc 99m pyrophosphate bone scanning in cardiac amyloidosis. *Arch Intern Med*. 1987;147:1039–44. <https://doi.org/10.1001/archinte.147.6.1039>.
- Castano A, Haq M, Narotsky DL, Goldsmith J, Weinberg RL, Morgenstern R, et al. Multicenter study of planar technetium 99m pyrophosphate cardiac imaging: predicting survival for patients with ATTR cardiac amyloidosis. *JAMA Cardiol*. 2016;1:880–9. <https://doi.org/10.1001/jamacardio.2016.2839>.
- Quock TP, Yan T, Chang E, Guthrie S, Broder MS. Epidemiology of AL amyloidosis: a real-world study using US claims data. *Blood Adv*. 2018;2:1046–53. <https://doi.org/10.1182/bloodadvances.2018016402>.
- Cornwell GG, Murdoch WL, Kyle RA, Westermark P, Pitkänen P. Frequency and distribution of senile cardiovascular amyloid. A clinicopathologic correlation. *Am J Med*. 1983;75:618–23. [https://doi.org/10.1016/0002-9343\(83\)90443-6](https://doi.org/10.1016/0002-9343(83)90443-6).
- Tanskanen M, Peuralinna T, Polvikoski T, Notkola IL, Sulkava R, Hardy J, et al. Senile systemic amyloidosis affects 25% of the very aged and associates with genetic variation in alpha2-macroglobulin and tau: a population-based autopsy study. *Ann Med*. 2008;40:232–9. <https://doi.org/10.1080/07853890701842988>.
- Banyersad SM, Sado DM, Flett AS, Gibbs SD, Pinney JH, Maestrini V, et al. Quantification of myocardial extracellular volume fraction in systemic AL amyloidosis: an equilibrium contrast cardiovascular magnetic resonance study. *Circ Cardiovasc Imaging*. 2013;6:34–9. <https://doi.org/10.1161/CIRCIMAGING.112.978627>.
- Oda S, Utsunomiya D, Morita K, Nakaura T, Yuki H, Kidoh M, et al. Cardiovascular magnetic resonance myocardial T1 mapping to detect and quantify cardiac involvement in familial amyloid polyneuropathy. *Eur Radiol*. 2017;27:4631–8. <https://doi.org/10.1007/s00330-017-4845-5>.
- Kotecha T, Martinez-Naharro A, Treibel TA, Francis R, Nordin S, Abdel-Gadir A, et al. Myocardial edema and prognosis in amyloidosis. *J Am Coll Cardiol*. 2018;71:2919–31. <https://doi.org/10.1016/j.jacc.2018.03.536>.
- Ridouani F, Damy T, Tacher V, Derbel H, Legou F, Sifaoui I, et al. Myocardial native T2 measurement to differentiate light-chain and transthyretin cardiac amyloidosis and assess prognosis. *J Cardiovasc Magn Reson*. 2018;20:58. <https://doi.org/10.1186/s12968-018-0478-3>.
- Gillmore JD, Maurer MS, Falk RH, Merlini G, Damy T, Dispenzieri A, et al. Nonbiopsy diagnosis of cardiac transthyretin amyloidosis. *Circulation*. 2016;133:2404–12. <https://doi.org/10.1161/CIRCULATIONAHA.116.021612>.

15. Ruberg FL, Miller EJ. Nuclear tracers for transthyretin cardiac amyloidosis: time to bone up? *Circ Cardiovasc Imaging*. 2013;6:162–4. <https://doi.org/10.1161/CIRCIMAGING.113.000178>.
16. Coutinho MC, Cortez-Dias N, Cantinho G, Conceição I, Oliveira A, Bordalo e Sá A, et al. Reduced myocardial 123-iodine meta-iodobenzylguanidine uptake: a prognostic marker in familial amyloid polyneuropathy. *Circ Cardiovasc Imaging*. 2013;6:627–36. <https://doi.org/10.1161/CIRCIMAGING.112.000367>.
17. Lee SP, Lee ES, Choi H, Im HJ, Koh Y, Lee MH, et al. ¹¹C-Pittsburgh B PET imaging in cardiac amyloidosis. *JACC Cardiovasc Imaging*. 2015;8:50–9. <https://doi.org/10.1016/j.jcmg.2014.09.018>.
18. Park MA, Padera RF, Belanger A, Dubey S, Hwang DH, Veeranna V, et al. ¹⁸F-florbetapir binds specifically to myocardial light chain and transthyretin amyloid deposits: autoradiography Study. *Circ Cardiovasc Imaging*. 2015;8: e002954. <https://doi.org/10.1161/CIRCIMAGING.114.002954>.
19. Law WP, Wang WY, Moore PT, Mollee PN, Ng AC. Cardiac amyloid imaging with ¹⁸F-florbetaben PET: a pilot study. *J Nucl Med*. 2016;57:1733–9. <https://doi.org/10.2967/jnumed.115.169870>.
20. Fine NM, Arruda-Olson AM, Dispenzieri A, Zeldenrust SR, Gertz MA, Kyle RA, et al. Yield of noncardiac biopsy for the diagnosis of transthyretin cardiac amyloidosis. *Am J Cardiol*. 2014;113:1723–7. <https://doi.org/10.1016/j.amjcard.2014.02.030>.
21. Quarta CC, Gonzalez-Lopez E, Gilbertson JA, Botcher N, Rowczenio D, Petrie A, et al. Diagnostic sensitivity of abdominal fat aspiration in cardiac amyloidosis. *Eur Heart J*. 2017;38:1905–8. <https://doi.org/10.1093/eurheartj/ehx047>.
22. Ren C, Ren J, Tian Z, Du Y, Hao Z, Zhang Z, et al. Assessment of cardiac amyloidosis with ^{99m}Tc-pyrophosphate (PYP) quantitative SPECT. *EJNMMI Phys*. 2021;8:3. <https://doi.org/10.1186/s40658-020-00342-7>.

Publisher's Note Springer Nature remains neutral with regard to jurisdictional claims in published maps and institutional affiliations.

Springer Nature or its licensor (e.g. a society or other partner) holds exclusive rights to this article under a publishing agreement with the author(s) or other rightsholder(s); author self-archiving of the accepted manuscript version of this article is solely governed by the terms of such publishing agreement and applicable law.